World Academy of Science, Engineering and Technology
International Journal of Mechanical and Mechatronics Engineering
Vol:7, No:5, 2013

Numerical Investigation of the Effect of Flow and Heat Transfer of a Semi-Cylindrical Obstacle Located in a Channel

Omer F. Can and Nevin Celik

***Abstract*—**In this study, a semi-cylinder obstacle placed in a channel is handled to determine the effect of flow and heat transfer around the obstacle. Both faces of the semi-cylinder are used in the numerical analysis. First, the front face of the semi-cylinder is stated perpendicular to flow, than the rear face is placed. The study is carried out numerically, by using commercial software ANSYS 11.0. The well-known κ-ε model is applied as the turbulence model. Reynolds number is in the range of 10^4 to 10^5 and air is assumed as the flowing fluid. The results showed that, heat transfer increased approximately 15 % in the front faze case, while it enhanced up to 28 % in the rear face case.

***Keywords*—**External flow, semi-cylinder obstacle, heat transfer, friction.

I. Introduction

THE flow past an obstacle has been a major research topic in fluid mechanics, not only because of the geometric effect, but also because of practical importance in engineering. Especially if there is heat transfer, between the obstacle and the fluid, the topic gains great importance. For that, the flow over a simple geometry, such as a circular cylinder or a sphere has often been investigated numerically and experimentally, and so there are numerous articles in the literature.

In most of the articles, in order to enhance the heat transfer, the geometry of the obstacle was optimized. The mostly analyzed geometries were triangles [1-7], rectangle blocks [8-10], and some other rectilinear protruding elements [11-17].

Both natural and mixed convections were analyzed in the obstructed channel flows. For example, Bakkas et al [8, 9] investigated the natural convection using rectangular blocks with a uniform heat flux. Dogan and Sivrioglu [11, 12] investigated natural convection heat transfer in an obstructed horizontal channel.

The geometry of the obstacle on which an external flow passes has great importance. We will focus on two rarely-used geometries; a front face of semi –cylinder, and rear-face of a semi-cylinder. Therefore, the following analysis examines steady, incompressible turbulent flow passing (i) a semi-cylinder placed in a channel at right angle to the oncoming fluid, and then passing (ii) the inverted semi-cylinder. Just for reading facility, we will call those two cases; *Case 1* and *Case 2*. The channel flow without any obstacle is also analyzed for comparisons, which is called *Case 0*.

O. F. Can is with the Dicle University, Department of Mechanical Engineering, Diyarbakir, Turkey (e-mail: ofcan@hotmail.com).

N. Celik, is with Firat University, Department of Mechatronics Engineering, Elazig, Turkey (e-mail:nevincelik23@gmail.com).

A. Method

Numerical analysis is carried out by using ANSYS-CFX 11.0 software package [19]. CFX is one of many available commercial software codes for executing Computational Fluid Dynamics (CFD) calculations. The code consists of four separate but connected components. In CFX –Workbench the geometry is created. The geometry is meshed with the aid of CFX-Mesh. The boundary conditions are applied in CFX-Pre. Also included in CFX-Pre is the solver control in which the solver is chosen as well as the convergence criteria. Then CFX-Solve is used to obtain the solution.

The fluid flow is assumed steady, incompressible and 2-D. A key parameter to predict the flow and heat transfer characteristics of this external flow is the Reynolds number, which is based on cylinder diameter (*D*), kinematic viscosity of the air (ν) and mean velocity of the fluid (*U*). For high values of *Re* such as 10^4-10^5 the flow is turbulent and air is used as the flowing fluid (*Pr* =0.701).The κ-ε model which is the best-known turbulence model involving additional differential equations is used as the turbulence model. The turbulence intensity is 10 %.

B. Governing Equations

To solve the problem three sets of equations; continuity, momentum and energy equations are required. In this study, simple algorithm is used for the finite volume approach [18]. The *z* component of Navier-Stokes equations is missed since the flow is 2-D.

Continuity

$$\frac{\partial u}{\partial x}+\frac{\partial v}{\partial y}=0 \tag{1}$$

x- momentum

$$\left(\frac{\partial(uu)}{\partial x}+\frac{\partial(uv)}{\partial y}\right)=-\frac{\partial\bar{P}}{\partial x}+\frac{1}{Re}\left(1+\frac{\nu_t}{\nu}\right)\nabla^2 u \tag{2}$$

y -momentum equation

$$\left(\frac{\partial(uv)}{\partial x}+\frac{\partial(vv)}{\partial y}\right)=-\frac{\partial\bar{P}}{\partial y}+\frac{1}{Re}\left(1+\frac{\nu_t}{\nu}\right)\nabla^2 v \tag{3}$$

Energy equation

$$u\frac{\partial T}{\partial x}+v\frac{\partial T}{\partial y}=\frac{1}{RePr}\left(1+\frac{\alpha_t}{\alpha}\right)\nabla^2 T \tag{4}$$

κ and ε equations for κ-ε model are [19, 20]

$$u\frac{\partial \kappa}{\partial x}+v\frac{\partial \kappa}{\partial y}=\frac{1}{Re}\left(\frac{\nu_t}{\sigma_k}\right)\nabla^2 \kappa + P - \varepsilon \tag{5}$$

$$u\frac{\partial \varepsilon}{\partial x}+v\frac{\partial \varepsilon}{\partial y}=\frac{1}{Re}\left(\frac{\nu_t}{\sigma\varepsilon}\right)\nabla^2 \varepsilon - C_1 S_\varepsilon - \rho C_2\frac{\varepsilon^2}{\kappa} \tag{6}$$

where P in Eq.(5) means the production of turbulent kinetic energy [20].

Wall friction coefficient, local Nusselt number and average Nusselt number were found as [2]

$$C_f = \frac{\tau_s}{\rho u_m^2/2} \tag{7}$$

$$Nu(x) = \left.\frac{\partial T^*}{\partial y^*}\right|_{y^*=0} \tag{8}$$

$$\overline{Nu} = \frac{\int_0^L Nu(x)dx}{L} \tag{9}$$

where T* = (T(x,0) - T∞)/Tc - T∞), and y* = y/L represent dimensionless temperature and dimensionless distance respectively [2].

C. Physical Model and Boundary Conditions

In Fig. 1(a), the flow passing the front face of a semi-cylinder is seen, which is already called *Case 1*. The flow passing an inverted semi-cylinder or rear side of the semi-cylinder, named *Case 2*, is seen in Fig 1(b).

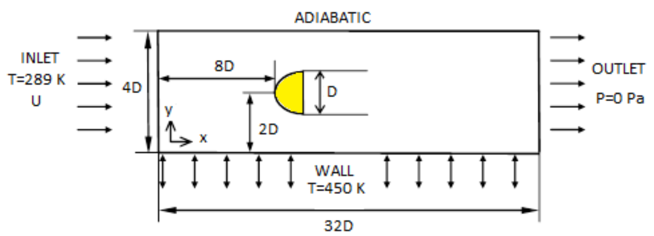

(a)

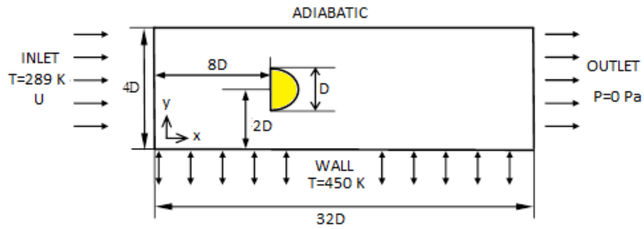

(b)

Fig. 1 Physical models, (a) *Case 1*, (b) *Case 2*

Three views of mesh structure of *Case 2* are presented in Fig. 2. For an appropriate solution, the mesh must be very sensitive. So mesh accuracy is obtained after three tests. The number of the elements and nodes for *Cases 1*, *2* and *0* are listed in Table I. In addition to the mesh knowledge the y+ values are also presented in Table I. In this study, y+ distance which is an important parameter for turbulent flow is taken into account. The first element's height of wall is assumed to be equal to 1. For the turbulent flows, usually for y+< 5 more sensitive results can be obtained. The y+ values, dimensionless distance between mesh and wall is presented in the last column at Table I.

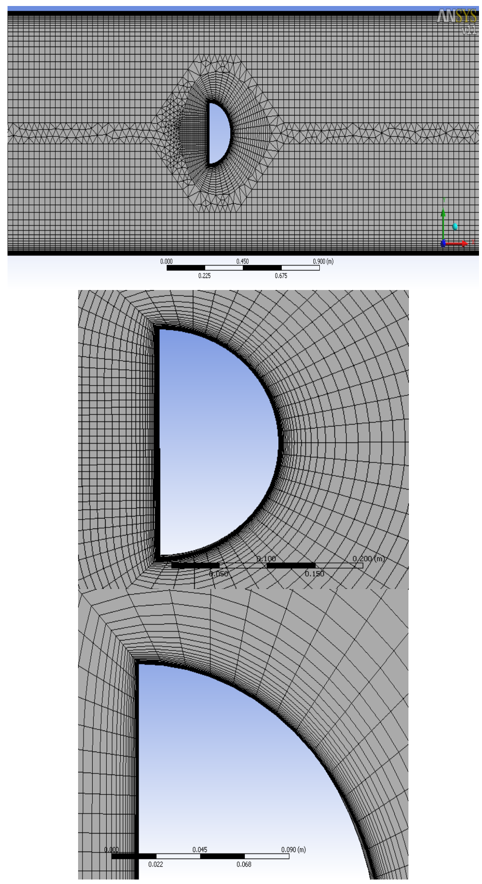

Fig. 2 Mesh model for Case 2

TABLE I
INFORMATION ABOUT THE MESH STRUCTURE

Cases	Element	Node	layer number on the walls	height of first element on the walls	y+
Case 0	26430	52236	50	2.401×10^{-5}	1
Case 1	22371	43892	50	2.035×10^{-5}	1
Case 2	29267	57702	50	2.392×10^{-5}	1

At the inlet of the solution domain, a uniform velocity is imposed. The distance from the entrance of the channel to the obstacles is 8*D*, total length of the channel is 32*D*. The temperature of the air at the inlet is considered as $T = 289$ K.

The upper wall of the channel is assumed adiabatic, while the bottom wall has 450 K constant temperature. Wall boundary condition is applied to the borders of the obstacle. The exit of the channel is outlet and therefore has zero static pressure.

II. RESULTS AND DISCUSSIONS

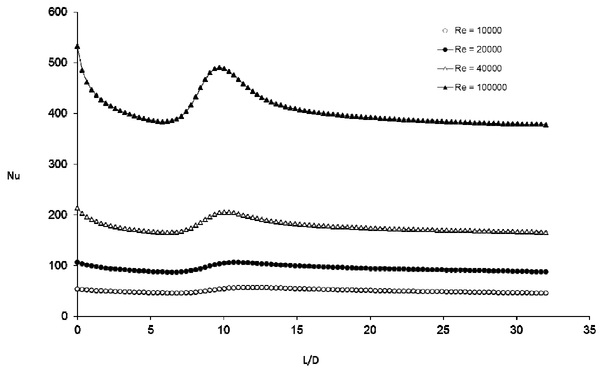

Fig. 3 Variation of Nu numbers versus Re numbers for *Case 1*

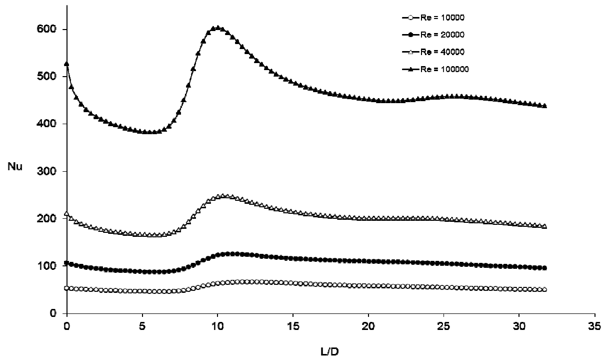

Fig. 4 Variation of Nu numbers versus Re numbers for *Case 2*

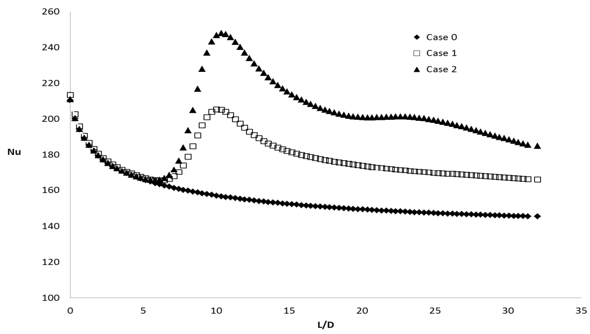

Fig. 5 Comparison of Nu numbers at $Re = 40000$

As already mentioned, for verification *Case 0* is handled. Fig. 3 represents the variation of local *Nu* along the channel length (*L/D*) for various Reynolds numbers, when *Case 1* is used as the obstacle. Similarly, Fig. 4 shows the *Nu* versus *L/D* variations with respect to *Re*, for *Case 2*.

As expected, local *Nu* numbers have a sharp increase around the obstacle ($L/D \geq 8$) for both cases. The highest local *Nu* is observed at $L/D \geq 10$ which represents the upper side of the obstacles because local *Nu* increases with increasing turbulence level on the upper side of the obstacle. The effect of the geometry affects the turbulence level, so does the heat transfer. It is clear that, *Case 2* has much more high heat transfer than *Case 1* has. Fig. 5 shows the comparisons of local *Nu*s for both *Cases 1* and *2* and also the empty channel case (*Case 0*).

Through the channel at $L/D \leq 8$, because of the absence of any obstacle, local *Nu* gradually decreases due to the transfer of heat transfer from fluid and wall. For the same reason, *Nu* reaches minimum value at the exit of the channel. Because of the unsteady flow around the obstacle, the effects of turbulence is the highest as previously mentioned. Also the vortices consisting at the rear of the obstacle are effective on the heat transfer.

The average *Nu* numbers, $\overline{\mathrm{Nu}}$ are presented by a listing table. Table II shows the $\overline{\mathrm{Nu}}$ values for all testes cases. Case 2 has the highest $\overline{\mathrm{Nu}}$ as expected from the local values.

TABLE II
VARIATION OF AVERAGE NUSSELT NUMBER VERSUS REYNOLDS NUMBER

Re	*Case 0*	*Case 1*	*Case 2*
10000	43.87	50.16	55.46
20000	82.14	94.64	105.25
40000	155.94	177.50	199.54
100000	359.16	407.63	464.02

In Fig. 6, variation of local wall friction coefficients, C_f. Are presented. For Case 0, the friction gradually decreases along the channel wall. However, when Case 1 or 2 is considered, a sharp increase generates. This is because the more resistance encounters exposure with obstacles of fluid. *Case 2* has higher wall coefficient C_f than *Case 1* has, because, the fluid after striking to front stagnation point will be more effective than the flow at radial direction.

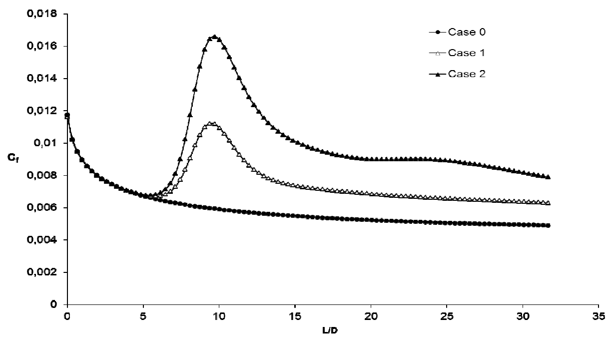

Fig. 6 Comparisons of wall friction coefficient at Re = 40000

The average C_fs is presented by a listing table (Table III). The C_f increases with increasing Re numbers.

TABLE III
VARIATION OF AVERAGE WALL FRICTION COEFFICIENTS VERSUS REYNOLDS NUMBER

Re	*Case 0*	*Case 1*	*Case 2*
10000	0.00048	0.00063	0.00077
20000	0.00168	0.00219	0.00274
40000	0.00580	0.00750	0.00950
100000	0.03038	0.03834	0.05051

Finally the velocity contours are presented to have a better understanding about the flow around the obstacles. The contour plots are presented in Fig. 7.

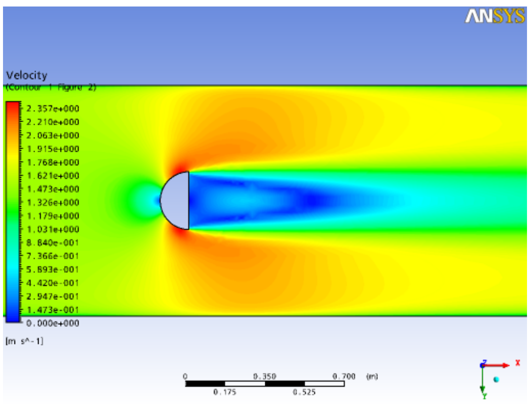

(a)

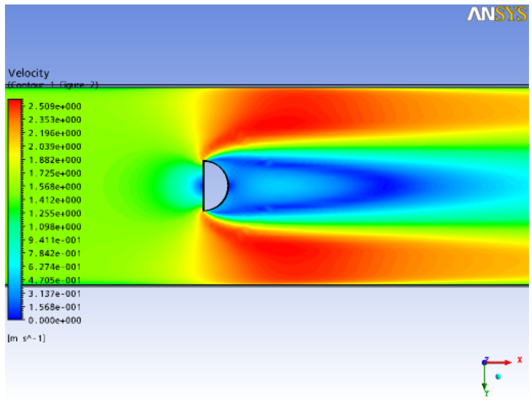

(b)

Fig. 7 Velocity contours for a) Case 1, b) Case 2

It is clearly seen in Fig. 7 that, the back side of the obstacles has low-velocity areas. Although the *Case 2* has a larger low-velocity area, it has high velocity areas especially at the up and down sides. These plots explain why higher heat transfer is observed for *Case 2*.

REFERENCES

[1] H. Abbassi, S. Turki, S. B. Nasrallah, "Numerical investigation of forced convection in a horizontal channel with a built-in triangular prism", *Journal of Heat Transfer,* vol. 124 (3) , pp. 571-57, 2002.
[2] H. Chattopadhyay, "Augmentation of heat transfer in a channel using a triangular prism", *International Journal of Thermal Science,.* vol.46 (5), pp. 501-505, 2007.
[3] M. Ali, O. Zeitoun, A. Nuhait, "Forced convection heat transfer over horizontal triangular cylinder in cross flow", International Journal of Thermal Sciences, vol.50, pp. 106–114, 2011
[4] A. C. Benim, H. Chattopadhyay, A. Nahavandi, "Computational analysis of turbulent forced convection in a channel with a triangular prism", International Journal of Thermal Sciences, vol. 50, pp. 1973-1983, 2011
[5] S. J. Lee, C. Woo Park, "Surface-pressure variations on a triangular prism by porous fences in a simulated atmospheric boundary layer", Journal of Wind Engineering and Industrial Aerodynamics, vol.73, pp. 45-58, 1998.
[6] O. Zeitoun, M. Ali, A. Nuhait, "Convective heat transfer around a triangular cylinder in an air cross flow", International Journal of Thermal Sciences, vol. 50, pp. 1685-1697, 2011
[7] S. Srikanth, A. K. Dhiman, S. Bijjam, "Confined flow and heat transfer across a triangular cylinder in a channel", International Journal of Thermal Sciences, vol.49, pp. 2191-2200, 2010
[8] M. Bakkas, A. Amahmid, M. Hasnaoui, "Numerical study of natural convection heat transfer in a horizontal channel provided with rectangular blocks releasing uniform heat flux and mounted on its lower wall", Energy Conversion and Management, vol.49, pp. 2757–2766, 2008.
[9] M. Bakkas, A. Amahmid, M. Hasnaoui, "Steady natural convection in a horizontal channel containing heated rectangular blocks periodically mounted on its lower wall", Energy Conversion and Management, vol.47, pp. 509–528, 2006.
[10] M. Najam, A. Amahmid, M. Hasnaoui, M. El Alami, "Unsteady mixed convection in a horizontal channel with rectangular blocks periodically distributed on its lower Wall", International Journal of Heat and Fluid Flow, vol. 24, pp. 726–735, 2003.
[11] M. Dogan, M. Sivrioglu, "Experimental investigation of mixed convection heat transfer from longitudinal fins in a horizontal rectangular channel: In natural convection dominated flow regimes", Energy Conversion and Management, vol.50, pp. 2513–2521, 2009.
[12] M. Dogan, M. Sivrioglu, "Experimental investigation of mixed convection heat transfer from longitudinal fins in a horizontal

rectangular channel", International Journal of Heat and Mass Transfer, vol. 53, pp. 2149–2158, 2010

[13] A. Hamouche, R. Bessaih, "Mixed convection air cooling of protruding heat sources mounted in a horizontal channel", International Communications in Heat and Mass Transfer, vol. 36, pp. 841–849, 2009.

[14] D. Mouhtadi, A. Amahmid, M. Hasnaoui, R. Bennacer, "Natural convection in a horizontal channel provided with heat generating blocks: discussion of the isothermal blocks validity", Energy Conversion and Management, vol. 53, pp. 45–54, 2011

[15] A. Dogan, M. Sivrioglu, S. Baskaya, "Investigation of mixed convection heat transfer in a horizontal channel with discrete heat sources at the top and at the bottom", International Journal of Heat and Mass Transfe , vol.49, pp. 2652–2662, 2006.

[16] B. Premachandran, C. Balaji, "Conjugate mixed convection with surface radiation from a horizontal channel with protruding heat sources", International Journal of Heat and Mass Transfer vol.49, pp. 3568–3582, 2006.

[17] J. J. M. Sillekens, C. C. M. Rindt, A. A. V. Steenhoven, "Development of laminar mixed convection in a horizontal square channel with heated side walls", International Journal of Heat and Fluid Flow vol.19, pp. 270–281, 1998

[18] ANSYS 11.0 (Academic Teaching Introductory) command References and gui.

[19] S.V. Patankar, Numerical Heat Transfer and Fluid Flow, Hemisphere, Washington, DC, 1980.

[20] B.E. Launder, D.B. Spalding, Lectures in Mathematical Models of Turbulence, Academic Press, London, 1972W.-K. Chen, *Linear Networks and Systems* (Book style). Belmont, CA: Wadsworth, 1993.